Three Phase Transmission Line Fault Location Based on the Generalized Bergeron Model

Dayou Lu[1], *Student Member, IEEE*, Yu Liu[1,2,*], *Member, IEEE* and Xiaodong Zheng[2,3], *Member, IEEE*
1. School of Information Science and Technology, ShanghaiTech University, Shanghai, China, 201210
2. Key Laboratory of Control of Power Transmission and Conversion, Ministry of Education, Shanghai, China, 200240
3. Department of Electrical Power Engineering, Shanghai Jiao Tong University, Shanghai, China, 200240
*Email: liuyu@shanghaitech.edu.cn

Abstract: Accurate fault location technique minimizes the power outage time and operating costs. This paper proposed a three phase transmission line fault location scheme based on the generalized Bergeron model. Three phase instantaneous voltage and current measurements at two terminals of the line are required. Compared to traditional Bergeron model based fault location scheme, the proposed method does not need the assumption of geometrically symmetric transmission lines and works for arbitrary transmission line parameters. Numerical experiments demonstrate that the proposed generalized Bergeron model based method has higher accuracy compared to the traditional Bergeron model based method.

Key words: fault location, generalized Bergeron model, three phase transmission line model

I. INTRODUCTION

AFTER a transmission line fault is isolated, accurate line fault location techniques are valuable, since they can minimize the time that the utility crews spend in searching for the fault, and therefore can reduce the power outage time and operating costs of the power system. Transmission line fault location techniques can be classified into two categories: fault analysis based methods and traveling wave based methods.

A. Fault analysis based methods

Fault analysis based methods calculate the location of the fault by using the analytical relationship between the available measurements at terminals of the transmission line and the fault location of the fault. This relationship is usually derived from the physical laws that the transmission line of interest should obey. Fault analysis based methods can be further classified into frequency domain methods and time domain methods.

1) Frequency domain methods

Frequency domain methods utilize fundamental frequency phasor measurements to calculate the location of the fault. One group of classic frequency domain methods are the impedance based methods [1]. The calculated line impedance between one selected terminal of the line and the location of the fault is proportional to the distance between the terminal and the fault. The influence of fault impedance can be mitigated by using measurements at both terminals of the line. The main disadvantage of the impedance based methods is the strong assumptions of the transmission line models. Lumped parameter models (without shunt capacitance or with lumped capacitance at terminals of the line) as well as sequence transmission line models are usually adopted, which may result in compromised fault location accuracy.

To overcome the limitations of impedance based methods, researchers proposed some other frequency domain methods to consider fully distributed shunt capacitance [2] and three phase model [3] of the transmission line. Nevertheless, since the fundamental frequency phasor calculation filters out signals with other frequencies, frequency domain methods may be less accurate especially during system transients. As a result, these methods may require a relatively long data window during faults to ensure fault location accuracy.

2) Time domain methods

Time domain methods utilize instantaneous measurements instead of phasors to calculate the location of the fault. Consequently, time domain methods only require a short data window during faults. One group of time domain methods determine the fault location by solving the differential equations that describes the physical laws between terminal instantaneous measurements and the fault location [4,5]. The main disadvantage of these methods is that the lumped parameter models (simplified R-L circuit [4], single or multi section π-equivalent circuit [5]) are typically required to form the differential equations with the fault location as an unknown variable, compromising the accuracy of fault location.

To use more accurate models (distributed parameter models) in time domain methods, researchers proposed the voltage methods [6,7] that determine the fault location by calculating the voltage distributions through the whole transmission line. The effectiveness of these methods is based on the fact that the voltage at the location of the fault should be an extremum of the voltage distribution. These methods can vary according to different ways of calculating the voltage distribution. One way is to directly solve the partial differential equations of the transmission line using finite difference method [6], where the accuracy of the solution is dependent on the density of the selected mesh. Another way is to use the Bergeron model of the transmission line [8]. Instead of selecting meshes, the voltage at any given location can be directly obtained through the Bergeron model. When applied to three phase transmission lines, the present voltage methods are usually based on modal decomposition, such as Karrenbauer transformation, Clarke transformation, etc., to decouple the three phase transmission line into three independent single phase lines [9]. However, these transformations assume that the three phase line is geometric symmetry (the diagonal elements of the parameter matrices are the same and the off-diagonal elements of the parameter matrices are the same). This assumption may bring errors to fault location results.

This work is sponsored by National Nature Science Foundation of China (No. 51807119), Shanghai Pujiang Program (No. 18PJ1408100) and Key Laboratory of Control of Power Transmission and Conversion (SJTU), Ministry of Education (No. 2015AB04). Their support is greatly appreciated.

B. Traveling wave based methods

The traveling wave based methods [10] locate the fault by utilizing the propagation time of traveling waves. The propagation time can be calculated with single-ended or dual-ended measurements. Single-ended traveling wave based methods measure the time difference of the subsequent arrival of traveling waves at the local terminal to determine the fault location, including type A, C, E and F according to how the traveling wave is generated (the fault, an injected impulse, closing and opening of the breaker, respectively). Dual-ended traveling wave based methods measure the time difference of the arrival of traveling waves generated by fault at both terminals to determine the fault location, including types B and D according to how to synchronize the dual-ended measurements (sending stop signals and GPS clock, respectively). The main limitation of traveling wave based methods is the detection reliability of traveling waves. Since the intensity of traveling waves is highly dependent on fault inception time, the arrival time of traveling waves may not be accurately captured.

C. The proposed method

In this paper, a time domain fault analysis based method is proposed. Specifically, the generalized Bergeron model is introduced to calculate the voltage distribution through the line and determine the location of the fault. To describe three phase transmission line physical laws, unlike the existing Bergeron model which utilizes modal decomposition method to decouple the three phase network into three independent single phase networks, the proposed generalized Bergeron model directly deals with the fully coupled three phase network that does not need the assumption of the geometric symmetry and works for arbitrary parameter matrices. Consequently, the fault location method based on the generalized Bergeron model has a smaller error compared to that based on the traditional Bergeron model. The rest of the paper is organized as follows. Section II introduces the derivation of the generalized Bergeron model. Section III describes the proposed fault location method based on the generalized Bergeron model. Section IV demonstrates the simulation results of the proposed fault location method. Section V draws a conclusion.

II. Derivation of Generalized Bergeron Model of Three Phase Transmission Lines

The derivation of the traditional single phase Bergeron model consists of two steps. First, express the relationship among the instantaneous voltages and currents at two terminals of a lossless transmission line where the series resistance of the line is ignored. Second, the total series resistance is approximated as three lumped resistors to obtain the model of a lossy transmission line [8]. The traditional single phase Bergeron model is,

$$\begin{aligned} i_k(t) = {} & 1/Z \cdot u_k(t) - (1-h)/2 \cdot \left[1/Z \cdot u_m(t-\tau) + h \cdot i_m(t-\tau)\right] \\ & -(1+h)/2 \cdot \left[1/Z u_k(t-\tau) + h \cdot i_k(t-\tau)\right] \end{aligned} \quad (1)$$

where i_k and i_m are the currents flowing into the two terminals k and m, u_k and u_m are the terminals voltages, $Z = Z_0 + R/4$, $h = (Z_0 - R/4)/(Z_0 + R/4)$, Z_0 is the wave impedance, R is the total series resistance of the line, τ is the wave traveling time from one terminal to the other terminal.

In this section, the generalized Bergeron model of three phase transmission lines with arbitrary parameter matrices (without the aforementioned assumption for modal decomposition that the line is geometrically symmetric) is derived. Similar as single phase Bergeron model, the derivation of the generalized Bergeron model consists of two steps. First, derive the relationship among the instantaneous voltages and currents at two terminals of a lossless three phase transmission line. Second, derive the relationship of a lossy three phase transmission line with lumped resistors. Details are as follows.

A. Step 1: Derivation of lossless three phase lines

The equivalent circuit of a lossless three phase transmission line with two terminals k and m is shown in Figure 1. A section with infinitesimal length dx is considered. The distance between section dx and terminal k is x. $\boldsymbol{L}$ and $\boldsymbol{C}$ are arbitrary inductance matrix and capacitance matrix per unit length (the series resistance of line is ignored and will be considered in Step 2). $u_s(x,t)$ and $i_s(x,t)$ (s=a,b,c) are voltages and currents (flowing from k to m) at the location of x.

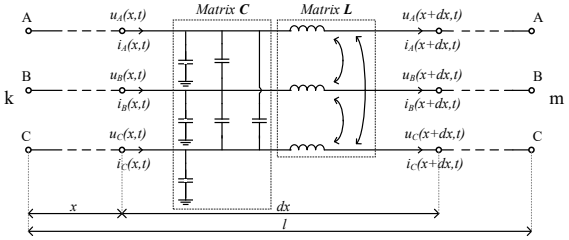

Figure 1. Equivalent circuit of a lossless three phase transmission line

The physical laws of the line can be described by partial differential equations:

$$\partial \boldsymbol{u}_{ABC}/\partial x = -\boldsymbol{L}\,\partial \boldsymbol{i}_{ABC}/\partial t \quad (2a)$$

$$\partial \boldsymbol{i}_{ABC}/\partial x = -\boldsymbol{C}\,\partial \boldsymbol{u}_{ABC}/\partial t \quad (2b)$$

where $\boldsymbol{u}_{ABC} = [u_A(x,t) \;\; u_B(x,t) \;\; u_C(x,t)]^T$, $\boldsymbol{i}_{ABC} = [i_A(x,t) \;\; i_B(x,t) \;\; i_C(x,t)]^T$.

From (2a) and (2b),

$$\partial^2 \boldsymbol{u}_{ABC}/\partial x^2 = \boldsymbol{LC} \cdot \partial^2 \boldsymbol{u}_{ABC}/\partial t^2 \quad (3)$$

Apply eigenvalue decomposition to matrix $\boldsymbol{LC}$, the eigenvalues are λ_1, λ_2 and λ_3, the corresponding eigenmatrix is $\boldsymbol{T}$. Define $\boldsymbol{u} = \boldsymbol{T}^{-1}\boldsymbol{u}_{ABC} = [u_1(x,t) \;\; u_2(x,t) \;\; u_3(x,t)]^T$ and $\boldsymbol{i} = \boldsymbol{T}^{-1}\boldsymbol{i}_{ABC} = [i_1(x,t) \;\; i_2(x,t) \;\; i_3(x,t)]^T$ as the mode voltages and mode currents (the voltage and current vectors without specific subscripts represent the mode vectors). Equation (3) can be transformed into mode model as follows (the subscripts j means the mode *1,2* and *3*, same for the rest of the paper),

$$\partial^2 u_j(x,t)/\partial x^2 = \lambda_j \cdot \partial^2 u_j(x,t)/\partial t^2 \quad (4)$$

The solution of (4) is shown as follows,

$$u_j = f_j\left(x + 1/\sqrt{\lambda_j} \cdot t\right) + g_j\left(x - 1/\sqrt{\lambda_j} \cdot t\right) \quad (5)$$

where f_j and g_j are functions which have second order continuous derivative.

Define $\boldsymbol{Q} = \left(\boldsymbol{T}^{-1}\boldsymbol{L}\boldsymbol{T}\right)^{-1}$ and transform (2a) into mode model,

$$\partial \boldsymbol{i}_{123}/\partial t = -\boldsymbol{Q} \cdot \partial \boldsymbol{u}_{123}/\partial x \quad (6)$$

From (5) and (6),

$$\boldsymbol{i}_{123}=\begin{bmatrix}\sqrt{\lambda_1} & & \\ & \sqrt{\lambda_2} & \\ & & \sqrt{\lambda_3}\end{bmatrix}\boldsymbol{Q}\begin{bmatrix}-f_1\left(x+1/\sqrt{\lambda_1}\cdot t\right)+g_1\left(x-1/\sqrt{\lambda_1}\cdot t\right)\\ -f_2\left(x+1/\sqrt{\lambda_2}\cdot t\right)+g_2\left(x-1/\sqrt{\lambda_2}\cdot t\right)\\ -f_3\left(x+1/\sqrt{\lambda_3}\cdot t\right)+g_3\left(x-1/\sqrt{\lambda_3}\cdot t\right)\end{bmatrix} \quad (7)$$

Define $\boldsymbol{B}=(diag([\lambda_1\ \ \lambda_2\ \ \lambda_3])\boldsymbol{Q})^{-1}$ where $diag([\cdot])$ means a diagonal matrix with the vector $[\cdot]$ as the diagonal elements. Compare (7) to (5),

$$\boldsymbol{Bi}+\boldsymbol{u}=2\begin{bmatrix}g_1\left(x-1/\sqrt{\lambda_1}\cdot t\right)\\ g_2\left(x-1/\sqrt{\lambda_2}\cdot t\right)\\ g_3\left(x-1/\sqrt{\lambda_3}\cdot t\right)\end{bmatrix} \quad (8)$$

Define travel times $\tau_j=l\cdot\sqrt{\lambda_j}$. Substitute $(x,t)=(0,t)$ and $(l,t+\tau_j)$ into (8):

$$\sum_{n=1}^{3}B_{jn}i_n(0,t)+u_j(0,t)=2g_j\left[-1/\sqrt{\lambda_j}\cdot t\right] \quad (9a)$$

$$\sum_{n=1}^{3}B_{jn}i_n\left(l,t+\tau_j\right)+u_j\left(l,t+\tau_j\right)=2g_j\left[l-1/\sqrt{\lambda_j}\cdot\left(t+\tau_j\right)\right] \quad (9b)$$

From the definition of τ_j, we can observe that the right hand sides of (9a) and (9b) are equal. After rewriting $u_j(0,t)=u_{kj}(t)$, $u_j(l,t)=-u_{mj}(t)$, $i_j(0,t)=i_{kj}(t)$ and $i_j(l,t)=-i_{mj}(t)$, the relationship among the voltages and currents at two terminals are shown as follows,

$$\sum_{n=1}^{3}B_{jn}i_{mn}(t)=u_{mj}(t)-\left[u_{kj}\left(t-\tau_j\right)+\sum_{n=1}^{3}B_{jn}i_{kn}\left(t-\tau_j\right)\right] \quad (10a)$$

Similarly, we have the following expressions by exchanging terminal k and m,

$$\sum_{n=1}^{3}B_{jn}i_{kn}(t)=u_{kj}(t)-\left[u_{mj}\left(t-\tau_j\right)+\sum_{n=1}^{3}B_{jn}i_{mn}\left(t-\tau_j\right)\right] \quad (10b)$$

Remark1: in the three phase generalized Bergeron model of lossless lines as described in (10), if the parameter matrices are arbitrary, we can observe that the voltages and currents of three modes are strongly coupled together.

B. Step 2: Derivation of lossy three phase lines

Next, the series resistance of the three phase transmission line is taken into account as follows. First, apply $\boldsymbol{T}^{-1}\boldsymbol{RT}$ to the total resistance matrix $\boldsymbol{R}$ and take the diagonal elements R_j as total series resistance of three modes, respectively. Here we assume that the off-diagonal elements of matrix $\boldsymbol{T}^{-1}\boldsymbol{RT}$ are small and have little effects on the modeling accuracy to reduce the model complexity. Afterwards for each mode, similar as the traditional Bergeron method, put lumped resistors $R_j/4$ at both ends of the line and $R_j/2$ at the middle of the line to approximate the fully distributed resistance.

The equivalent circuit of mode j with lumped resistors is shown in Figure 2. The nodes 1 and 6 represents the two terminals of the lossy transmission line of interest. The branches 2-3 and 4-5 represent lossless transmission lines with length $l/2$. The voltages and currents are defined in the figure.

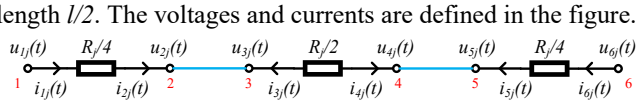

Figure 2. Equivalent circuit of mode j transmission line with 2 sections and 3 lumped series resistors

Remark 2: for the model shown in Figure 2, the three modes of the resistors (branch 1-2, 3-4 or 5-6) are fully decoupled, while the three modes of the lossless lines (branch 2-3 or 4-5) are strongly coupled.

The task is to find the relationship among the instantaneous voltages and currents at nodes 1 and 6 (u_{1j}, i_{1j}, u_{6j} and i_{6j}). First, find the relationship among voltages and currents at nodes 2 and 5 (u_{2j}, i_{2j}, u_{5j} and i_{5j}). Use (10a) for the lines 2-3 and 4-5, and consider the middle resistor,

$$\sum_{n=1}^{3}B_{jn}i_{2j}(t)=u_{2j}(t)-\frac{R_j}{2}i_{4j}\left(t-\frac{\tau_j}{2}\right)-u_{5j}\left(t-\tau_j\right)-\sum_{n=1}^{3}B_{jn}i_{5j}\left(t-\tau_j\right) \quad (11)$$

In (11), the only term that is not expressed by the voltages and currents at nodes 2 and 5 is $i_{4j}\left(t-\tau_j/2\right)$. Therefore, we want to first express i_{4j} using i_{5j} and u_{5j}. In general, this is to express i_{kj} using i_{mj} and u_{mj} for lossless line *k-m*. This relationship can be derived by combining (10a) and (10b),

$$\begin{aligned}i_{kj}(t)=X_j\Bigg[&u_{mj}\left(t+\tau_j\right)-\sum_{n=1}^{3}B_{jn}i_{mn}\left(t+\tau_j\right)-u_{mj}\left(t-\tau_j\right)\\ &-\sum_{n=1}^{3}B_{jn}i_{mn}\left(t-\tau_j\right)\Bigg]-Y_j\Bigg[u_{m(j+1)}\left(t+\tau_{(j+1)}\right)-\sum_{n=1}^{3}B_{(j+1)n}i_{mn}\left(t+\tau_{(j+1)}\right)\\ &-u_{m(j+1)}\left(t-\tau_{(j+1)}\right)-\sum_{n=1}^{3}B_{(j+1)n}i_{mn}\left(t-\tau_{(j+1)}\right)\Bigg]+Z_j\Bigg[u_{m(j+2)}\left(t+\tau_{(j+2)}\right)\\ &-\sum_{n=1}^{3}B_{(j+2)n}i_{mn}\left(t+\tau_{(j+2)}\right)-u_{m(j+2)}\left(t-\tau_{(j+2)}\right)-\sum_{n=1}^{3}B_{(j+2)n}i_{mn}\left(t-\tau_{(j+2)}\right)\Bigg]\end{aligned} \quad (12)$$

where $X_j=\frac{C_jB_{(j+1)(j+2)}-D_jB_{j(j+2)(j+2)}}{2\left(C_jE_j-D_jF_j\right)}$, $Y_j=\frac{C_jB_{j(j+2)}}{2\left(C_jE_j-D_jF_j\right)}$, $Z_j=\frac{D_jB_{j(j+2)}}{2\left(C_jE_j-D_jF_j\right)}$, $C_j=\left(B_{(j+2)(j+2)}B_{j(j+1)}-B_{j(j+2)}B_{(j+2)(j+2)}\right)$, $D_j=\left(B_{(j+1)(j+2)}B_{j(j+1)}-B_{j(j+2)}B_{(j+1)(j+1)}\right)$, $E_j=\left(B_{(j+1)(j+2)}B_{jj}-B_{j(j+2)}B_{(j+1)j}\right)$, $F_j=\left(B_{(j+2)(j+2)}B_{jj}-B_{j(j+2)}B_{(j+2)j}\right)$ and for simplicity, the subscripts $(j+x)$ $(x=1,2)$ means the mode $(j+x\text{-}3)$ if $j+x>3$ (same for the rest of the paper).

In addition, the voltages and currents at nodes 1,2 and 6,5 obey the following equations,

$$i_{2j}(t)=i_{1j}(t),\quad u_{2j}(t)=u_{1j}(t)-R_j/4\cdot i_{1j}(t) \quad (13a)$$

$$i_{5j}(t)=i_{6j}(t),\quad u_{5j}(t)=u_{6j}(t)-R_j/4\cdot i_{6j}(t) \quad (13b)$$

Substitute (12) and (13) to (11), the generalized Bergeron model of lossy three phase transmission lines with arbitrary parameters, which describes the relationship among the voltages and currents at nodes 1 and 6, is provided,

$$\begin{aligned}&\sum_{n=1}^{3}M_{jn}i_{1n}(t)=u_{1j}(t)-u_{6j}\left(t-\tau_j\right)-\sum_{p=n}^{3}N_{jn}i_{6n}\left(t-\tau_j\right)\\ &-R_jX_j/2\cdot\left[u_{6j}(t)-\sum_{n=1}^{3}M_{jn}i_{6n}(t)-u_{6j}\left(t-\tau_j\right)-\sum_{n=1}^{3}N_{jn}i_{6n}\left(t-\tau_j\right)\right]\\ &+R_jY_j/2\cdot\Bigg\{u_{6(j+1)}\left[t+\left(\tau_{(j+1)}-\tau_j\right)/2\right]-\sum_{n=1}^{3}M_{(j+1)n}i_{6n}\left[t+\left(\tau_{(j+1)}-\tau_j\right)/2\right]\\ &-u_{6(j+1)}\left[t-\left(\tau_{(j+1)}+\tau_j\right)/2\right]-\sum_{n=1}^{3}N_{(j+1)n}i_{6n}\left[t-\left(\tau_{(j+1)}+\tau_j\right)/2\right]\Bigg\}\\ &-R_jZ_j/2\cdot\Bigg\{u_{6(j+2)}\left[t+\left(\tau_{(j+2)}-\tau_j\right)/2\right]-\sum_{n=1}^{3}M_{(j+2)n}i_{6n}\left[t+\left(\tau_{(j+2)}-\tau_j\right)/2\right]\\ &-u_{6(j+2)}\left[t-\left(\tau_{(j+2)}+\tau_j\right)/2\right]-\sum_{n=1}^{3}N_{(j+2)n}i_{6n}\left[t-\left(\tau_{(j+2)}+\tau_j\right)/2\right]\Bigg\}\end{aligned} \quad (14a)$$

where $\boldsymbol{M}=\boldsymbol{B}+\boldsymbol{R}_{123}/4$, $\boldsymbol{N}=\boldsymbol{B}-\boldsymbol{R}_{123}/4$, $\boldsymbol{R}_{123}=diag([R_1\ \ R_2\ \ R_3])$.

Similarly, equation (14b) can be derived by exchanging terminals 1 and 6 (the equation is shown on the next page).

III. Fault Location Method

This section introduces the way of using the three phase generalized Bergeron model to locate faults. First, for each terminal, the voltage distribution through the line is calculated from local instantaneous voltages and currents (by assuming that the line is fault free, starting from the local terminal).

Second, the intersection point of two voltage distributions

calculated from two terminals is the fault location. In this section, the way of calculating instantaneous voltages with one terminal voltages and currents is first derived. Afterwards, the fault location algorithm is introduced.

$$\begin{aligned}&\sum_{n=1}^{3}M_{jn}i_{6n}(t)=u_{6j}(t)-u_{1j}(t-\tau_j)-\sum_{p=n}^{3}N_{jn}i_{1n}(t-\tau_j)\\&-R_jX_j/2\cdot\left[u_{1j}(t)-\sum_{n=1}^{3}M_{jn}i_{1n}(t)-u_{1j}(t-\tau_j)-\sum_{n=1}^{3}N_{jn}i_{1n}(t-\tau_j)\right]\\&+R_jY_j/2\cdot\left\{u_{1(j+1)}\left[t+\left(\tau_{(j+1)}-\tau_j\right)/2\right]-\sum_{n=1}^{3}M_{(j+1)n}i_{1n}\left[t+\left(\tau_{(j+1)}-\tau_j\right)/2\right]\right.\\&\left.-u_{1(j+1)}\left[t-\left(\tau_{(j+1)}+\tau_j\right)/2\right]-\sum_{n=1}^{3}N_{(j+1)n}i_{1n}\left[t-\left(\tau_{(j+1)}+\tau_j\right)/2\right]\right\}\\&-R_jZ_j/2\cdot\left\{u_{1(j+2)}\left[t+\left(\tau_{(j+2)}-\tau_j\right)/2\right]-\sum_{n=1}^{3}M_{(j+2)n}i_{1n}\left[t+\left(\tau_{(j+2)}-\tau_j\right)/2\right]\right.\\&\left.-u_{1(j+2)}\left[t-\left(\tau_{(j+2)}+\tau_j\right)/2\right]-\sum_{n=1}^{3}N_{(j+2)n}i_{1n}\left[t+\left(\tau_{(j+2)}-\tau_j\right)/2\right]\right\}\end{aligned}\tag{14b}$$

A. Derivation of voltage distributions

This section first derives the way of calculating voltages at one terminal with voltages and currents at the other terminal. Next, the voltage distributions through the line can be obtained by simply setting different length of the transmission line.

In (14b), define $U_{6j}(t)$ as follows,

$$\begin{aligned}&U_{6j}(t)=\sum_{j=1}^{3}M_{1j}i_{6j}(t)-u_{61}(t)=-u_{1j}(t-\tau_j)-\sum_{n=1}^{3}N_{jn}i_{1n}(t-\tau_j)\\&-R_jX_j/2\cdot\left[u_{1j}(t)-\sum_{n=1}^{3}M_{jn}i_{1n}(t)-u_{1j}(t-\tau_j)-\sum_{n=1}^{3}N_{jn}i_{1n}(t-\tau_j)\right]\\&+R_jY_j/2\cdot\left\{u_{1(j+1)}\left[t+\left(\tau_{(j+1)}-\tau_j\right)/2\right]-\sum_{n=1}^{3}M_{(j+1)n}i_{1n}\left[t+\left(\tau_{(j+1)}-\tau_j\right)/2\right]\right.\\&\left.-u_{1(j+1)}\left[t-\left(\tau_{(j+1)}+\tau_j\right)/2\right]-\sum_{n=1}^{3}N_{(j+1)n}i_{1nj}\left[t-\left(\tau_{(j+1)}+\tau_j\right)/2\right]\right\}\\&-R_jZ_j/2\cdot\left\{u_{1(j+2)}\left[t+\left(\tau_{(j+2)}-\tau_j\right)/2\right]-\sum_{n=1}^{3}M_{(j+2)n}i_{1n}\left[t+\left(\tau_{(j+2)}-\tau_j\right)/2\right]\right.\\&\left.-u_{1(j+2)}\left[t-\left(\tau_{(j+2)}+\tau_j\right)/2\right]-\sum_{n=1}^{3}N_{(j+2)n}i_{1n}\left[t+\left(\tau_{(j+2)}-\tau_j\right)/2\right]\right\}\end{aligned}\tag{15}$$

Note that $\boldsymbol{M}+\boldsymbol{N}=2\boldsymbol{B}$, so the right hand side of (14a) can be rewritten with the definition of $U_{6j}(t)$ and the expression with $\boldsymbol{B}$ (except $u_{1j}(t)$). $\tau_j/2$ are added to the three modes equations for the matrix manipulation. Equation (14a) is rewritten as follows,

$$\begin{aligned}&2\left(1-R_jX_j/2\right)\sum_{n=1}^{3}B_{jn}i_{6n}\left(t-\tau_j/2\right)+R_jY_j\sum_{n=1}^{3}B_{(j+1)n}i_{6n}\left(t-\tau_{(j+1)}/2\right)\\&-R_jZ_j\sum_{n=1}^{3}B_{(j+2)n}i_{6n}\left(t-\tau_{(j+2)}/2\right)=u_{1j}\left(t+\tau_j/2\right)-\sum_{n=1}^{3}M_{jn}i_{1n}\left(t+\tau_j/2\right)\\&+U_{6j}\left(t-\tau_j/2\right)-R_jX_j/2\cdot\left[-U_{6j}\left(t+\tau_j/2\right)+U_{6j}\left(t-\tau_j/2\right)\right]\\&+R_jY_j/2\cdot\left[-U_{6(j+1)}\left(t+\tau_{(j+1)}/2\right)+U_{6(j+1)}\left(t-\tau_{(j+1)}/2\right)\right]\\&-R_jZ_j/2\cdot\left[-U_{6(j+2)}\left(t+\tau_{(j+2)}/2\right)+U_{6(j+2)}\left(t-\tau_{(j+2)}/2\right)\right]\end{aligned}\tag{16}$$

Define the right hand sides of (16) as $V_{6j}(t)$. Rewrite (16) into the matrix form, the current vector $\boldsymbol{i_6(t)}=\left[i_{6,1}(t)\quad i_{6,2}(t)\quad i_{6,3}(t)\right]^T$ is,

$$\boldsymbol{i_6(t)}=\boldsymbol{B}^{-1}\begin{bmatrix}G_{11}V_{61}\left(t+\tau_1/2\right)+G_{12}V_{62}\left(t+\tau_1/2\right)+G_{13}V_{63}\left(t+\tau_1/2\right)\\G_{21}V_{61}\left(t+\tau_2/2\right)+G_{22}V_{62}\left(t+\tau_2/2\right)+G_{23}V_{63}\left(t+\tau_2/2\right)\\G_{31}V_{61}\left(t+\tau_3/2\right)+G_{32}V_{62}\left(t+\tau_3/2\right)+G_{33}V_{63}\left(t+\tau_3/2\right)\end{bmatrix}\tag{17}$$

where $\boldsymbol{G}=\begin{bmatrix}2\left(1-R_1X_1/2\right)&R_1Y_1&-R_1Z_1\\-R_2Z_2&2\left(1-R_2X_2/2\right)&R_2Y_2\\R_3Y_3&-R_3Z_3&2\left(1-R_3X_3/2\right)\end{bmatrix}^{-1}$.

Define $\boldsymbol{U_6(t)}=\left[U_{61}(t)\quad U_{62}(t)\quad U_{63}(t)\right]^T$. The voltage vector $\boldsymbol{u_6(t)}=\left[u_{61}(t)\quad u_{62}(t)\quad u_{63}(t)\right]^T$ is,

$$\boldsymbol{u_6(t)}=\boldsymbol{Mi_6(t)}-\boldsymbol{U_6(t)}\tag{18}$$

From (15) to (17), we can observe that $\boldsymbol{i_6(t)}$ and $\boldsymbol{U_6(t)}$ are only determined by the voltages and currents at terminal 1. Therefore, equation (18) can be utilized to calculate the voltage distributions through the line.

B. Fault Location Algorithm

After using (18) to obtain the voltage distributions $u_{1x}(x,t)$ and $u_{6x}(x,t)$ from node 1 and nodes 6, the intersection point of $u_{1x}(x,t)$ and $u_{6x}(x,t)$ is the location of the fault. Here we use the voltage distributions of the faulted phases as an example (the phase voltage can be directly obtained from the mode voltages). If the fault includes multiple phases, the fault location is estimated as the average fault location results from each phase. To find the intersection point of $u_{1x}(x,t)$ and $u_{6x}(x,t)$ is equivalent to finding x such that $\left|u_{1x}(x,t)-u_{6x}(x,t)\right|$ is equal to zero at all samples. Considering inaccurate measurements and models in actual systems, we can find the lowest point at the below curve as the fault location to improve accuracy [7].

$$f(x)=\sum_{t=t_1}^{t_2}\left|u_{1x}(x,t)-u_{6x}(x,t)\right|\tag{19}$$

where (t_1,t_2) is the summation time window.

Remark3: for the traditional Bergeron model based fault location method, the voltage distributions are calculated using the traditional Bergeron model (with geometrically symmetric assumptions) instead of (18). However, after obtaining the voltage distributions, the fault location algorithm is similar. The summation time window in (19) is selected to be 3 ms after the fault occurs.

IV. Simulation Results

The example test system of a 500-kV two-machine system with a 300 km transmission line is shown in Figure 3. The frequency-dependent parameters for the transmission line model are considered in the simulation. The sources parameters and the line parameters are shown in Tables 1 and 2, respectively. Three phase instantaneous voltage and current measurements are installed at both terminals of the line. The sampling interval is 10μs.

Due to space limitations, here we will only show the results of three groups of events, low impedance 0.1 ohm phase A to G faults, high impedance 100 ohm phase A to G faults and high impedance 200 ohm phase A to G faults. In each group of events, the proposed generalized Bergeron model based fault location method is compared to the traditional Bergeron model based fault location method.

A. Event Group 1: 0.1 ohm phase A to G faults

A 0.1 ohm phase A to G fault occurs at 150km from the left side. The $f(x)$ curves with the generalized Bergeron model and the traditional Bergeron method are shown in Figure 4 (a). The fault location result with the generalized Bergeron model is 0.2 km, while the fault location result with the traditional Bergeron model is 3 km. We can observe that the proposed method is more accurate than the traditional method.

To further validate the effectiveness of the proposed algorithm, 0.1 ohm phase A to G faults through the line are

tested. The results are depicted in Figure 4(b). We can observe that the proposed method has lower fault location error compared to traditional method.

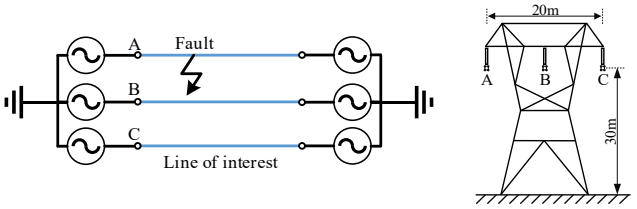

(a) Test system (b) Tower structure

Figure 3. Simulation model

Table 1. Sources parameters

	Left source	Right source
Source reactance	3.1+j31.4 (ohm)	3.1+j31.4 (ohm)
Voltage RMS value	500 (kV)	500 (kV)
Frequency	50 (Hz)	50 (Hz)
Initial phase	0 (°)	0 (°)

Table 2. Conductors parameters

Outer radius	0.0203454 (m)
Total number of strands	19
Total number of outer strands	12
Strands radius	0.003
DC resistance	0.03206(ohm/km)
Sag (all conductors)	10(m)
Total bundled sub-conductors	4
Sub-conductor spacing	0.4572(m)

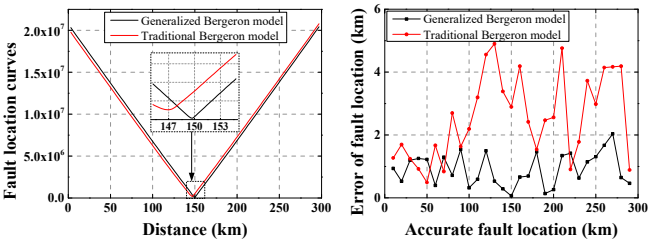

(a) Specific fault at 150 km (b) Faults through the line

Figure 4. Comparison between the proposed method and the traditional method, 0.1 ohm A to G faults

B. *Event Group 2: 100 ohm phase A to G faults*

100 ohm phase A to G faults through the line are tested. The results are depicted in Figure 5 (a). We can observe that the proposed method has lower fault location error compared to the traditional method.

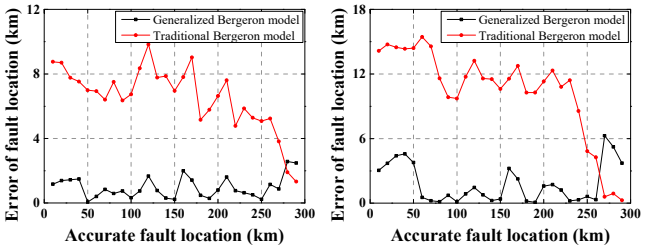

(a) 100 ohm faults (b) 200 ohm faults

Figure 5. Comparison between the proposed method and the traditional method, high impedance A to G faults through the line

C. *Event Group 3: 200 ohm phase A to G faults*

200 ohm phase A to G faults through the line are tested. The results are depicted in Figure 5 (b). We can observe that the proposed method has lower fault location error compared to the traditional method.

D. *Discussions*

From the results, we can conclude that the proposed method has better accuracy compared to the traditional method. This is due to the fact that the proposed method fully considers the characteristics that brought by the asymmetry of tower structures. Nevertheless, for the proposed method, it can be seen that the fault location error can still be up to 2% during a high impedance fault. This is due to the fact that this generalized Bergeron model did not consider the frequency-dependent parameters of the line, which could potentially generate errors especially during system transients. The way of considering frequency-dependent parameters will be included in future publications.

V. Conclusion

This paper proposes a three phase transmission line fault location method using the generalized Bergeron model. Unlike traditional Bergeron model based fault location methods, the proposed method does not require geometrically symmetric assumptions and works for transmission lines with arbitrary parameter matrices. The paper first derives a generalized Bergeron model to describe the relationship among the voltages and currents at two terminals of a lossy three phase transmission line. Afterwards, the proposed fault location method based on the generalized Bergeron model is introduced. Simulation results prove that the proposed method has better accuracy compare to the traditional method.

References

[1] Das, S., Santoso, S., Gaikwad, A., et al.: 'Impedance-based fault location in transmission networks: theory and application', IEEE Access, pp. 537–557, Feb. 2014.

[2] Y. Liu, Y. An and B. Xie: "State Estimation Based Transmission Line Fault Locating with Sequence Distributed Parameter Models", IEEE Conference on Energy Internet and Energy System Integration (EI2), 2017.

[3] Y. Liu, Z. Tan and J. Xie: "Phasor Domain Transmission Line Fault Locating with Three Phase Distributed Parameter Modeling", IEEE Power and Energy Society (PES) General Meeting, 2018.

[4] Samantaray, S. R., L. N. Tripathy and P. K. Dash: "Differential equation-based fault locator for unified power flow controller-based transmission line using synchronised phasor measurements", Iet Generation Transmission and Distributionc 3.1:86-98, 2008.

[5] Y. Liu, S. Meliopoulos, Z. Tan, L. Sun and R. Fan: "Dynamic State Estimation-Based Fault Locating on Transmission Lines", IET Generation, Transmission & Distribution, VOL. 11, NO. 17, pp. 4184-4192, Nov. 2017.

[6] A. Gopalakrishnan, M. Kezunovic, S. M. McKenna, and D. M. Hamai: 'Fault Location Using the Distributed Parameter Transmission Line Model', IEEE Trans. on Power Delivery, VOL. 15, NO. 4, Oct. 2000.

[7] Guobing Song, Jiale Suonan, Qingqiang Xu, Ping Chen, and Yaozhong Ge: 'Parallel Transmission Lines Fault Location Algorithm Based on Differential Component Net', IEEE Trans. on Power Delivery, VOL. 20, NO. 4, Oct. 2005.

[8] Hermann W. Dommel: 'Digital Computer Solution of Electromagnetic Transients in Single- and Multiphase Networks', IEEE Trans. on Power Apprartus and Systems, VOL. PAS-88, NO. 4, Apr. 1969.

[9] Ou Junzhang, Zhang Zhonghui: 'The Research of Fault Location of Transmission Line Based on Bergeron Model', 2010 3rd International Conference on Advanced Computer Theory and Engineering(ICACTE), 2010.

[10] IEEE Standard C37.114: 'IEEE guide for determining fault location on AC transmission and distribution lines', 2014.